Fibers and Polymers 2017, Vol.18, No.11, 2070-2078
DOI 10.1007/s12221-017-7215-7

ISSN 1229-9197 (print version)
ISSN 1875-0052 (electronic version)

Removal of Some Cationic Dyes from Aqueous Solution by Acrylamide- or 2-hydroxyethyl Methacrylate-based Copolymeric Hydrogels

Yasemin Işikver*

Department of Chemistry, Faculty of Science, Cumhuriyet University, Sivas 58140, Turkey

(Received March 8, 2017; Revised July 24, 2017; Accepted August 26, 2017)

Abstract: In this study, anionic hydrogels were prepared using a crosslinker (N,N′-methylenebisacrylamide) through a free radical addition reaction in aqueous solutions of neutral acrylamide or 2-hydroxyethyl methacrylate monomer and anionic monomers, mesaconic acid or aconitic acid. Cationic dyes along with safranine (azine-), nile blue (oxazine-) and methylene blue (thiazine-) were selected as models of pollutants, and adsorption of these dyes onto the hydrogels was investigated. To examine the effect of concentration on adsorption, dye solutions prepared with a concentration range of 5-50 mg l^{-1} and 0.1 g hydrogel at 25 °C were exposed to the hydrogels until equilibrium was established. Dye adsorption onto the hydrogels was found to be an *L* type Giles adsorption isotherm. Monolayer sorption capacity and adsorption constant values were calculated from the Langmuir plots. To calculate R_L values, a non-dimensional analysis was used and they were always found to be $0<R<1$. In other words, the hydrogels were favorable for adsorption of these dyes. Aqueous solutions of dyes were observed to interact with hydrogels in the following order: oxazine > azine > thiazine. Furthermore, the higher the number of carboxyl groups in the hydrogel composition, the higher the adsorbed amount of substance.

Keywords: Adsorption, Aconitic acid, 2-hydroxyethyl methacrylate, Mesaconic acid

Introduction

Dyes or pigments are widely used in the health, textile, paint, paper and printing industries. It is possible to see how effluents from these industries affect the color of wastewater. For example, in the paint industry, the amount of paint that remains in the effluent determines how severely the chemistry of living organisms will be affected. Colored wastewater reduces the transparency of the aquatic environment to light. Additionally, oxidation reactions and degradation of the colored matter in aquatic environments can give rise to toxic and carcinogenic compounds. Therefore, the treatment of wastewater is of great ecological importance.

Treatment of wastewater using various physical/chemical methods such as flocculation/coagulation, adsorption, and chemical oxidation can remove compounds that affect biological systems. The removal efficiency varies depending on the type and amount of contaminants in the wastewater, which makes it more difficult to choose the most appropriate method [1-3]. However, adsorption is one of the most common and effective methods for removal of dyes. The most widely used adsorbents are activated carbon, zeolite, and bentonite. There are recent studies that have been carried out using composite materials or artificial adsorbents. Crosslinked hydrogels that contain functional groups such as amine, hydroxyl, carboxyl, and sulfonyl are preferably used as adsorbents for removing dyes from aqueous solutions [4-10].

Acar *et al*. investigated the usage of depolymerization products of waste PET for removal of cationic dyes (Brilliant Green and Safranine T) from aqueous solutions. The effects of contact time and initial dye concentration on adsorption process were studied. In addition, adsorption data were evaluated using Langmuir and Freundlich adsorption isotherm models [11].

Şolpan *et al*. described the preparation and color-removal ability of a novel series of polymeric adsorbents. In this work studied the ability of poly(AAm-co-AAc) hydrogels to adsorb cationic dyes from aqueous solution under several experimental conditions [12].

Bajpai *et al*. studied an effective removal of methylene blue dye using poly(methacrylic acid) hydrogel as a potential adsorbent [13].

Mohy Eldin *et al*. investigated the equilibrium, kinetics, and thermodynamics of the removal of methylene blue (MB) ions from an aqueous solution using amidoxime PAN-grafted cotton fabrics. Moreover, stimulation studied performed to investigate the MB diffusion and exchange process in the amidoxime PAN-grafted cotton fabrics [14].

This study investigated the preparation of acrylamide (AAm)- or 2-hydroxyethyl methacrylate (HEMA)-based anionic copolymers and characterizes them through fourier transform infrared spectroscopy (FTIR), scanning electron microscope (SEM) and thermal gravimetric (TG) analyses. It also investigated the use of these compounds for the removal of azine (safranin), oxazin (nile blue) and thiazine (methylene blue) group cationic dyes.

Experimental

Chemicals

Acrylamide (AAm), 2-hydroxyethyl methacrylate (HEMA), mesaconic acid (MeA), N,N'-methylenebisacrylamide (NNMBA) and ammonium persulfate (APS) were purchased from Merck (Germany). Aconitic acid (AcA) and N,N,N',N'-

---

*Corresponding author: caldiran@cumhuriyet.edu.tr

Table 1. Some properties of the dyes

Dye	Chemical structure	Molar mass	Colour index Nr.
Safranine	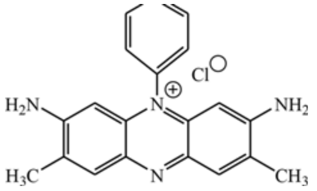	350.84	502240
Nil Blue	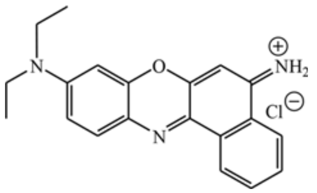	353.85	51180
Methylene Blue	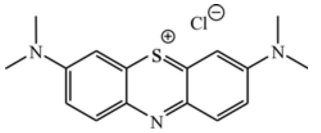	319.85	52015

tetramethylethylenediamine (TEMED) were obtained from Sigma/Aldrich (USA). Safranine, nile blue and methylene blue were purchased from Merck (Germany). Double-distilled water was used throughout the investigation.

Synthesis of Hydrogels

Acrylamide (AAm; 0.9 mol), carboxylic acid monomers (MeA or AcA; 0.1 mol) and N, N′-methylenebisacrylamide (NNMBA; 0.05 mol) were dissolved in water. Then 0.005 mol of ammonium persulfate and 0.005 mol of N,N,N′,N′-tetramethylethylenediamine were added. The mixture was placed into PVC straws. The hydrogels were prepared in thermostated water bath at 25 °C. After 24 hours, the hydrogels were removed from the straws, cut into pieces 3-4 mm in length, washed with distilled water and then dried in air and vacuum. The hydrogels were used in powder form. HEMA-based hydrogels were synthesized using the same method.

Characterization

FTIR spectra of the hydrogels (KBr pellets) were prepared using a FTIR Mattson-1000 spectrophotometer in the 4000-400 cm^{-1} range.

TG and DSC thermograms of the hydrogels were recorded through a Shimadzu-50 model thermal analyzer. Thermal tests were performed using a sample mass of 5-10 mg under a nitrogen atmosphere at a scan rate of 10 °C min^{-1}.

Surface morphology of the hydrogels was investigated through a scanning electron microscope (Tescan-Mira 3). The specimens were made conductive by coating with Au-Pd in a sputter coater device before SEM investigations. SEM images of the hydrogels were taken at 20.00 KX magnifying values.

Adsorption Studies

To examine the effect of dye concentration on adsorption, dye solutions were prepared at a concentration range of 5 to 50 mg l^{-1}, and then 0.1 g of dry hydrogel transferred into 50 ml of aqueous solutions of dye and allowed to equilibrate for 24 h at 25 °C. The adsorption isotherms were generated after determining the amount of dyes adsorbed from the solutions.

To examine the effect of temperature on adsorption, 0.1 g of dry polymer was placed in dye solutions at a concentration of 25 mg l^{-1} and maintained for 24 hours at 25, 30, 35, 40 and 45 °C. Besides, the amount of dyes adsorbed onto the hydrogels (q) at each temperature was calculated.

The adsorption of safranine, nile blue, and methylene blue solutions was recorded at wavelengths of 519, 638.5, and 663 nm, respectively, using a Shimadzu A160 model UV-VIS spectrophotometer.

Results and Discussion

Synthesis of Hydrogels

AAm-based anionic hydrogels were prepared using NMMBA as a crosslinker through a free radical addition reaction in aqueous solutions of neutral AAm monomer, and also anionic monomers such as MeA with 2 carboxyl groups or AcA with 3 carboxyl groups. These hydrogels were designated as P(AAm-co-MeA) and P(AAm-co-AcA).

The copolymerization reaction was initiated using the redox system ammonium persulfate and N,N,N',N'-tetramethylethylenediamine. The polymerization was carried out in PVC straws at 25 °C. After 24 hours, the hydrogels were removed from the straws, cut into pieces 3 to 4 mm in length, washed with distilled water and then dried in air and vacuum. The hydrogels were used in powder form.

HEMA-based anionic hydrogels were synthesized using the same method and designated as P(HEMA-co-MeA) and P(HEMA-co-AcA).

Characterization

FTIR Spectroscopy

FTIR spectra of the hydrogels (Figure 1) indicate the adsorption bands of AAm, HEMA, MeA, and AcA units. The bands in the region of 3200-3600 cm^{-1} are attributable to the O-H and N-H bands of a primary amine. The band at 1550 cm^{-1} is attributed to an O-H band related to a carbonyl group, and the bands at 1730 cm^{-1} characterize C=O groups in carboxylic acids. Finally, the bands at 1470 and 1380 cm^{-1} are related to -CH_2- groups on the chains [10,15-17].

Thermogravimetric Analysis

Initial degradation temperature (T_i), the temperature of maximum rate of change (T_{max}), final degradation temperature (T_f), the half-life temperature (T_h), the maximum decomposition rate (r_{max}) and the amount of the substance at the maximum

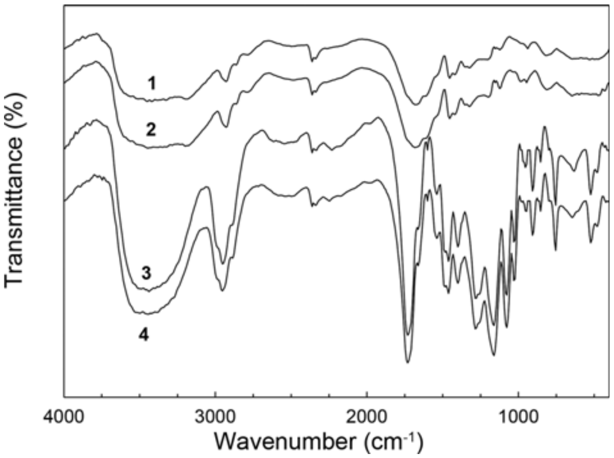

Figure 1. FTIR spectra of the hydrogels; (1) P(AAm-co-MeA), (2) P(AAm-co-AcA), (3) P(HEMA-co-MeA), and (4) P(HEMA-co-AcA).

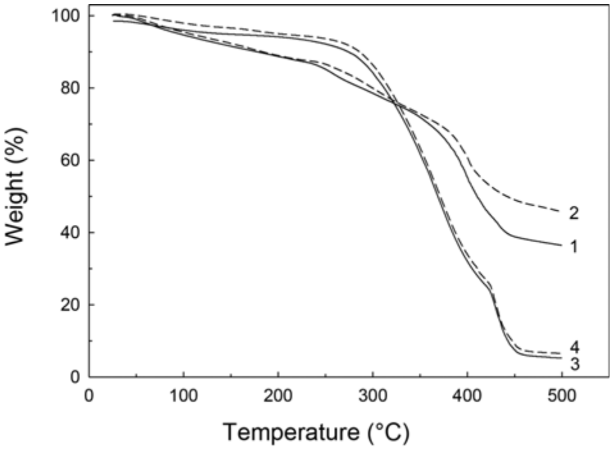

Figure 2. TG thermograms of.the hydrogels; (1) P(AAm-co-MeA), (2) P(AAm-co-AcA), (3) P(HEMA-co-MeA), and (4) P(HEMA-co-AcA).

rate of change (C_{max}) were determined from the TG curves in Figure 2. The results were given in Table 2.

The mass loss of the hydrogels took place in several steps. In the first step, the mass loss between 25 and 200 ^oC was caused by the loss of weakly bound water. The second step was decomposition of pendant -NH_2 and -COOH groups between 200 and 300 ^oC and the main chain breakdown between 300 and 420 ^oC. Finally, the mass loss that occurred between 420 and 500 ^oC was resulted from the carbonization of the hydrogels [18-21].

The T_i and T_f values of the anionic hydrogels that were made of mesaconic acid were found to be lower than those of the anionic hydrogels that were made of aconitic acid. This can be resulted from the concentration of -COOH groups in the hydrogels since less -COOH groups in the hydrogels led to a decrease in T_i and T_f values.

Differential Scanning Calorimetry

Glass transition temperatures (T_g) of the hydrogels were determined from the DSC curves in Figure 3. The results were given in Table 3.

T_g values of crosslinked PAAm and PHEMA homopolymers were 190 ^oC and 126 ^oC, respectively [16-20]. These values were higher than those of the P(AAm-co-MeA) and P(HEMA-co-MeA) copolymers (Figure 3). The reason for the increase in T_g could be copolymerization. T_g values of the P(AAm-co-MeA) and P(HEMA-co-MeA) hydrogels with 2 carboxyl groups were higher than those of the P(AAm-co-AcA) and P(HEMA-co-AcA) hydrogels with 3 carboxyl groups. The -COOH group in the structure of the polymer acts as plasticizers and the increasing number of these groups leads to a decrease in the T_g values [18-21].

Scanning Electron Microscopy

Figure 4 shows the SEM images of the hydrogels at 20,000× magnification. A quite regular and uniform characteristic surface structure was observed in the SEM images of the hydrogels. There were uniformly distributed local gaps on the hydrogel surfaces.

Table 2. The thermal degradation values of the hydrogels

Hydrogel	T_i (^oC)	T_m (^oC)	C_{max} (%)	r_{max} (mgmin^{-1})	T_f (^oC)	T_h (^oC)
P(AAm-co-MeA)						
1. peak	242	259	69	0.18	443	410
2. peak	368	399	65	0.58		
P(AAm-co-AcA)						
1. peak	248	298	74	0.20	449	440
2. peak	384	401	70	0.59		
P(HEMA-co-MeA)						
1. peak	289	370	70	0.50	448	370
2. peak	424	432	85	0.48		
P(HEMA-co-AcA)						
1. peak	291	373	63	0.52	450	372
2. peak	426	430	92	0.48		

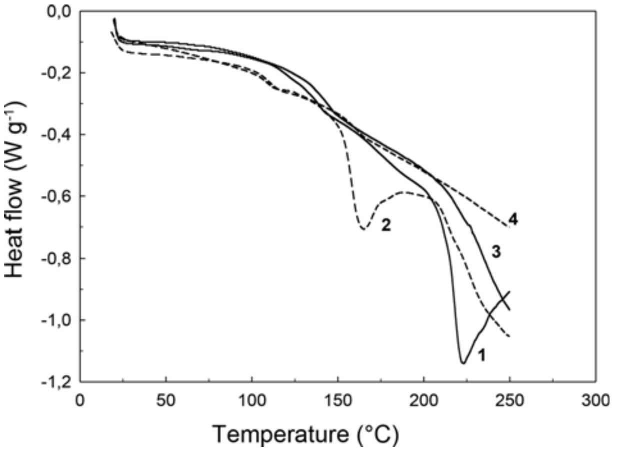

Figure 3. DSC thermograms of.the hydrogels; (1) P(AAm-co-MeA), (2) P(AAm-co-AcA), (3) P(HEMA-co-MeA), and (4) P(HEMA-co-AcA).

Table 3. Glass transition temperature (T_g) of the hydrogels

Hydrogel	T_g (^oC)
P(AAm-co-MeA)	206
P(AAm-AcA)	153
P(HEMA-MeA)	130
P(HEMA-AcA)	104

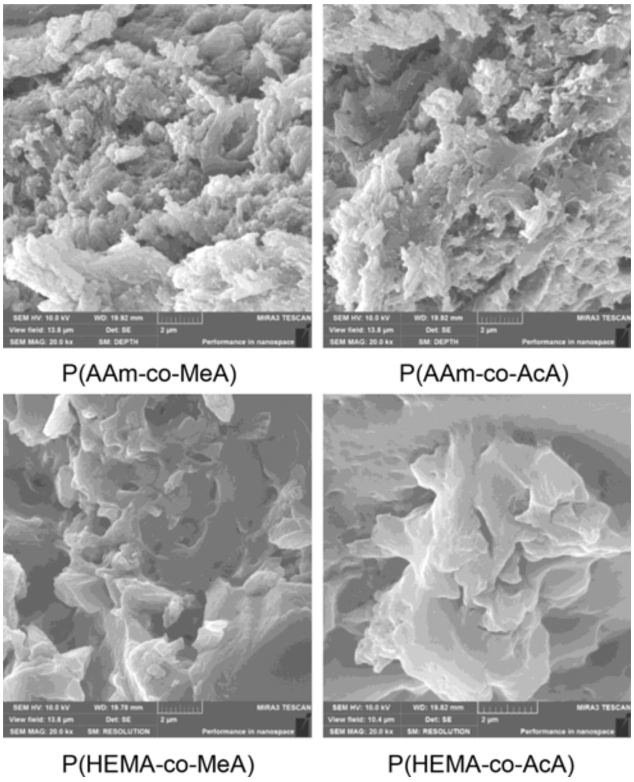
P(AAm-co-MeA) P(AAm-co-AcA)

P(HEMA-co-MeA) P(HEMA-co-AcA)

Figure 4. SEM images of the hydrogels (20.00 KX).

Adsorption Studies

The Concentration Effect on Adsorption

To examine the adsorption mechanism, hydrogels were placed in aqueous solutions of safranine, nile blue, and

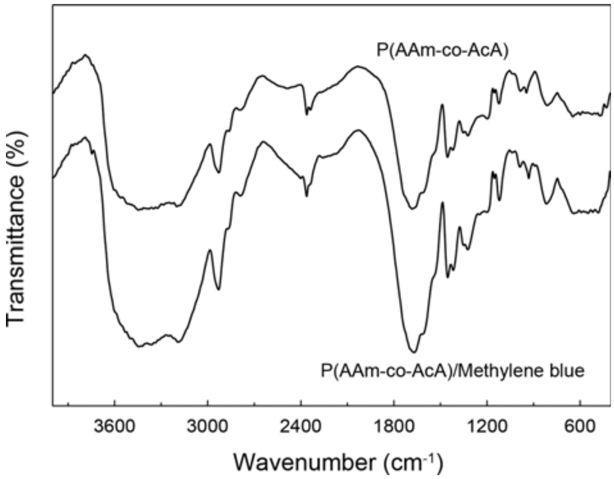

Figure 5. FTIR spectra of the hydrogels after adsorption of dyes.

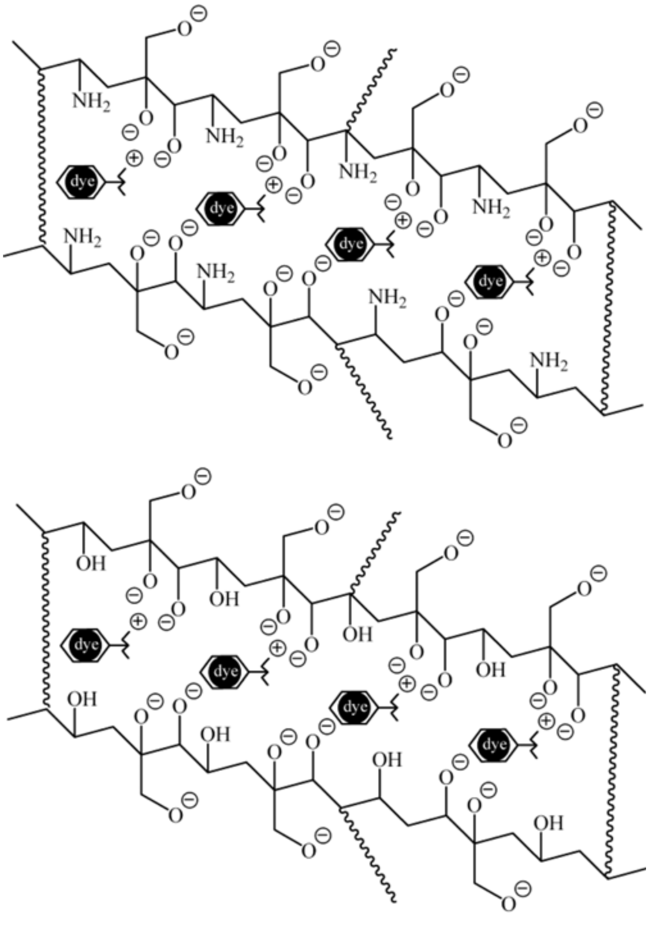

Figure 6. The possible interaction mechanisms of the dyes with the hydrogels.

methylene blue and they were left for a single-day equilibration process. FTIR spectra of the hydrogel/dye system in Figure 5 show the differences between P(AAm-co-AcA) and P(AAm-co-AcA)/methylene blue.

FT-IR spectra that were obtained before and after dye adsorption were compared and no change was observed in the specific bands associated with functional groups (1550 and 1730 cm^{-1}) indicating that dye adsorption onto the hydrogels was physical. Figure 6 indicates the possible interaction mechanisms.

PAAm and PHEMA are non-ionic polymers and generally do not interact with molecules. Anionic hydrogels including MeA or AcA monomers contain ionizable groups (-COOH). These negatively charged groups can interact with positively charged groups (cationic dyes) through electrostatic forces [22-27].

To examine the effect of dye concentration on adsorption, dye solutions were prepared with a concentration range from 5 to 50 mg l^{-1}, and then 0.1 g of dry hydrogel at 25 °C was exposed to these solutions for 24 hours was established.

In a batch adsorption system at equilibrium, the total dye concentration (C_o, mg l^{-1}) is as follows:

$$C_o = C_B + C \tag{1}$$

Here, C_B is the equilibrium concentration of the dye in the adsorbent (mg l^{-1}), and C is the equilibrium concentration of the dye in the solution (mg l^{-1}). The amount of dye adsorbed onto the hydrogels (q) was calculated from the equation (1), and equation (2).

$$q = \frac{C_B \cdot V}{m} \tag{2}$$

Here, V is the volume of solution (L) and m is the mass of the hydrogels (g).

Figure 7 shows the adsorption isotherms of the dye on AAm or HEMA based hydrogels. Dye adsorption onto the hydrogels was determined to be an L type Giles adsorption isotherm [28].

Langmuir Model

The Langmuir model describes a mono-layer adsorption process on a homogeneous surface. The Langmuir equation is represented by equation (3)

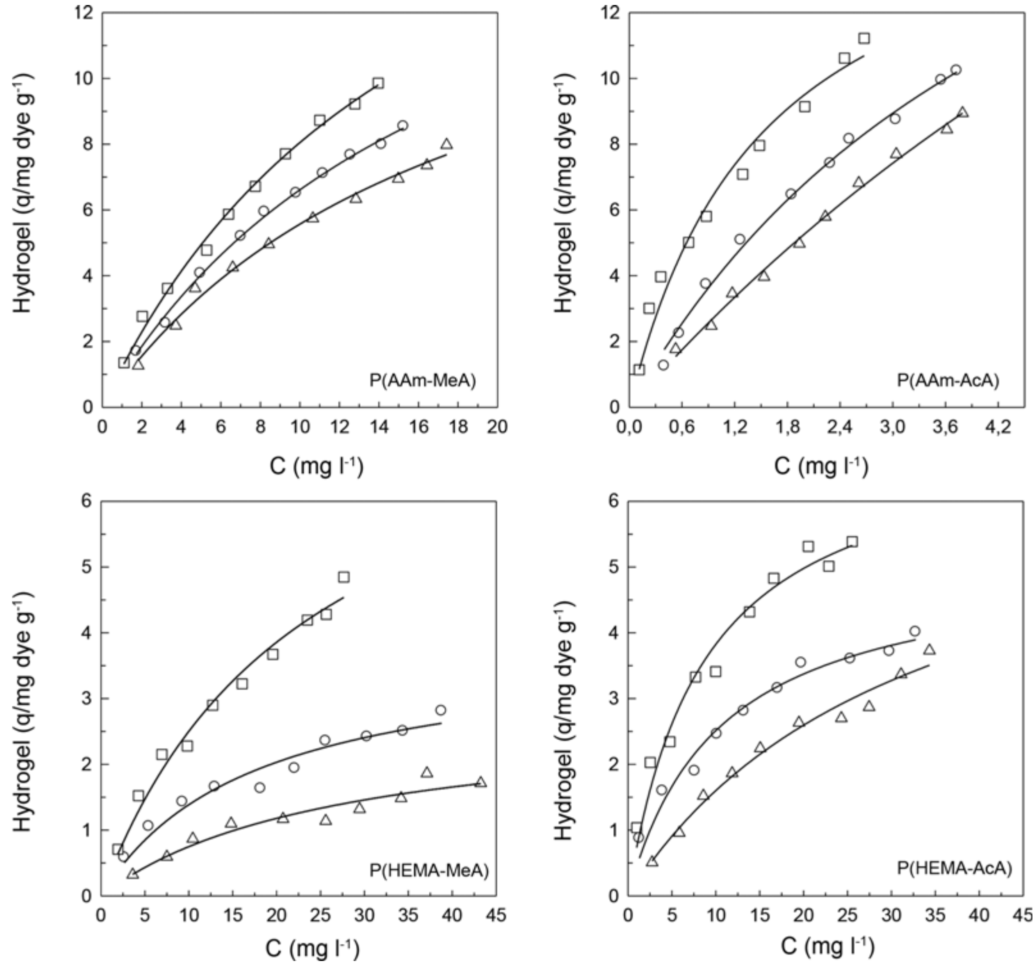

Figure 7. The binding isotherm of the hydrogel/dye system; □; Nile blue, ○; Safranine, △; methylene blue.

Table 4. Parameters for dye adsorption derived from Langmuir model

Hydrogel	Safranine			Nile Blue			Methylene Blue		
	X_L (mg g^{-1})	K_L (l mg^{-1})	R^2	X_L (mg g^{-1})	K_L (l mg^{-1})	R^2	X_L (mg g^{-1})	K_L (l mg^{-1})	R^2
P(AAm-co-MeA)	18.48	0.0557	0.9975	21.74	0.0558	0.9944	15.67	0.0551	0.9914
P(AAm-co-AcA)	24.02	0.1977	0.9943	16.86	0.6473	0.9758	39.59	0.0769	0.9950
P(HEMA-co-MeA)	3.803	0.0573	0.9516	8.429	0.0422	0.9797	2.777	0.0369	0.9243
P(HEMA-co-AcA)	5.135	0.0957	0.9730	7.133	0.1156	0.9704	6.865	0.0304	0.9797

$$q = \frac{X_L \cdot K_L \cdot C}{1 + K_L \cdot C} \tag{3}$$

Monolayer sorption capacity (X_L/mg g^{-1}) and adsorption constant (K_L/l mg^{-1}) values were calculated from the Langmuir plots using equation (3). These values were indicated in Table 4.

To predict whether the hydrogels were ‘favorable’ due to the non-dimensional factor (R_L), further consideration was given to Langmuir isotherms.

$$R_L = 1/(1 + K_L C) \tag{4}$$

Table 5 shows R_L values that were found using the non-dimensional analysis. The values were always in $0 < R < 1$ range, which meant the hydrogels were favorable for dye adsorption.

Further considerations of Langmuir parameters to predict the adsorbent doses (m/V as g l^{-1}) for the removal of 50 % the dyes from a hypothetic solution (50 mg l^{-1}) were calculated by using the following equation and indicated in Table 6.

$$\frac{m}{V} = \frac{C_o - C}{q} = \frac{C_o - C}{(K_L X_L C)/(1 + X_L C)} \tag{5}$$

The amount of the adsorbent to be used in terms of cost is important. The lower amount found for P(AAm-co-AcA) should be evidence for the cost effectiveness of this hydrogel.

Table 5. The values of R_L found from dimensionless analysis

Hydrogel	Safranine	Nile Blue	Methylene Blue
P(AAm-co-MeA)	0.263	0.264	0.266
P(AAm-co-AcA)	0.092	0.029	0.206
P(HEMA-co-MeA)	0.259	0.322	0.351
P(HEMA-co-AcA)	0.173	0.147	0.397

Table 6. The values of the adsorbent doses (m/V as g l^{-1})

Hydrogel	Safranine	Nile Blue	Methylene Blue
P(AAm-co-MeA)	1.4	1.1	1.6
P(AAm-co-AcA)	1.0	1.5	0.6
P(HEMA-co-MeA)	6.6	3.0	9.0
P(HEMA-co-AcA)	4.8	3.5	3.6

The removal efficiency (RE) to the hydrogels was calculated using equation (6).

$$RE\ \% = \frac{C_B}{C_o} \cdot 100 \tag{6}$$

Table 7 shows the removal efficiency from 50 mg l^{-1} of dye solutions to the hydrogels. This removal efficiency was indicated in the following order: methylene blue<safranine< nile blue.

Table 6 and 7 show that P(AAm-co-AcA) has the lowest adsorbent dose and the highest removal efficiency value in all the dyes.

The adsorbed amounts of dyes for AAm-based hydrogels were higher than those for HEMA-based hydrogels. Also, the adsorbed amounts of dyes for the hydrogels with 3 carboxyl groups were higher than those for the hydrogels with 2 carboxyl groups. Increased number of carboxyl groups, the primary effective sites for adsorption, in the adsorbent also led to an increase in adsorption capacity. P(AAm-co-AcA) and P(HEMA-co-AcA) hydrogels adsorbed higher amounts of the dyes than P(AAm-co-MeA) and P(HEMA-co-MeA) hydrogels did.

Dyes were observed to interact with hydrogels that were prepared using aqueous solutions of these dyes in the following order: oxazine>azine>thiazine.

This difference can be releated with the electronic (mesomeric and inductive) and steric effect of the substituents on the molecules of the dyes [35]. The mesomeric effect of the -NH_2 substituents in acrylamide leads to an increase in the polarity in the C=O group and to better adsorption compared to the HEMA-based hydrogels. In the HEMA monomer, the inductive effect of the methacrylate substituent is more dominant, and this effect reduces the interaction with the positively charged dye molecules.

Table 7. The removal efficiency values for adsorption of 50 mg l^{-1} dye solutions onto the hydrogels

Hydrogel	Safranine	Nile Blue	Methylene Blue
P(AAm-co-MeA)	69.5	72.1	65.0
P(AAm-co-AcA)	92.5	94.7	92.0
P(HEMA-co-MeA)	24.3	44.7	13.5
P(HEMA-co-AcA)	34.5	48.9	31.3

The positive charge on the nitrogen in nile blue increases the adsorption by interacting with the hydrogels more easily. The methylene blue contains a ring with positive charge on the nitrogen and sulfur atoms; the sulfur atom has a larger radius compared to that of the nitrogen. Therefore, the hydrogels and the methylene blue interact less and reduce the adsorption. In the Safranine molecule, the benzene ring on the positively charged nitrogen decreases the charge density, and it also impedes the adsorption with the hydrogels due to its steric effect.

To purpose of comparison, the results of our study and reported adsorption capacities in the literature before for the dyes on different low-cost adsorbents were given in Table 8.

These data can be interpreted that, the dye adsorption capacities of AAm- or HEMA- based anionic hydrogels for the dyes were compatible and comparable with the results of other adsorbents that have been given in the literature before. As a result, we can say that dye adsorption capacities of AAm- or HEMA- based anionic hydrogels can be workable for new potential and low cost adsorption systems.

Temkin Model

Temkin model, which assumes that the heat of adsorption of all molecules in the layer decreases linearly with coverage due to adsorbent-adsorbate interaction, was also applied to fit the experimental data. The linearized Temkin model can be described by equation (7).

$$\theta = \frac{RT}{\Delta Q}\ln K_o + \frac{RT}{\Delta Q}\ln C_d \tag{7}$$

where is the fraction coverage ($q=q/X_L$), R is the universal gas constant (8.314 J mol^{-1} K^{-1}), T is the temperature (K), ΔQ is the variation of adsorption energy (kJ mol^{-1}), and K_0 is the Temkin equilibrium constant (l mg^{-1}).

The ΔQ and the K_o values calculated from the Temkin isotherm for dye adsorption in the hydrogels are given in Table 9.

The variation of adsorption energy (ΔQ) is positive for all dyes and indicating that the adsorption is exothermic. This result indicates a weak interaction between adsorbent and adsorbate supporting a mechanism of electrostatic forces [36,37].

Temperature Effect on Adsorption

To determine the effect of temperature on adsorption, 0.1 g of dry polymer was placed in dye solutions at a concentration of 25 mg l^{-1} and maintained for 24 hours at 25, 30, 35, 40 and 45 °C. In addition, the amount of the dye adsorbed onto

Table 8. Maximum adsorption capacities for the dyes on different adsorbents

Adsorbent	Adsorbate	Maximum adsorption capacity (mg g^{-1})	Reference
Sulfonated phenolic resin	Safranine	103	29
Starch-g-acrylic acid copolymer 1	Safranine	116.5	30
Starch-g-acrylic acid copolymer 2		204	
PET depolymerization products	Safranine	29	11
Poly(AAm-co-AAc)	Safranine	(μmol/repeating unit) 3834	12
Bentonite	Methylene Blue	108	13
Zeolit		50	
Sepiolite	Methylene Blue	52	32
Polymethacrylic acid	Methylene Blue	150	13
Amidoxime PAN-g-cotton fabrics	Methylene Blue	22.27	14
AMPS/CTA-cotton	Methylene Blue	43.9	33
Acrylamide/Itaconic acid	Methylene Blue	(μmol/repeating unit) 513.1	34
	Nile Blue	(μmol/repeating unit) 593.3	
Sulfonated phenolic resin	Nil Blue	107	29
Acrylamide/Mesaconic acid	Nil Blue	(mol g^{-1}) 6.26·10^{-6}	8
Acrylamide/Maleic acid	Nil Blue	(μmol/repeating unit) 593.3	6
P(AAm-co-AcA)	Safranine Nil Blue Methylene Blue	24.02 16.86 39.59	This study

Table 9. Parameters for dye adsorption derived from Temkin model

Hydrogel	Safranine			Nile Blue			Methylene Blue		
	ΔQ (kJ mol^{-1})	K_o (l mg^{-1})	R	ΔQ (kJ mol^{-1})	K_o (l mg^{-1})	R	ΔQ (kJ mol^{-1})	K_o (l mg^{-1})	R
P(AAm-co-MeA)	56.39	1.28	0.987	24.46	1.07	0.975	45.88	1.40	0.988
P(AAm-co-AcA)	13.39	3.05	0.993	8.40	2.39	0.975	19.06	2.25	0.970
P(HEMA-co-MeA)	42.72	1.34	0.978	19.20	1.60	0.977	19.21	2.36	0.960
P(HEMA-co-AcA)	30.21	1.49	0.972	14.84	1.53	0.973	12.20	2.32	0.978

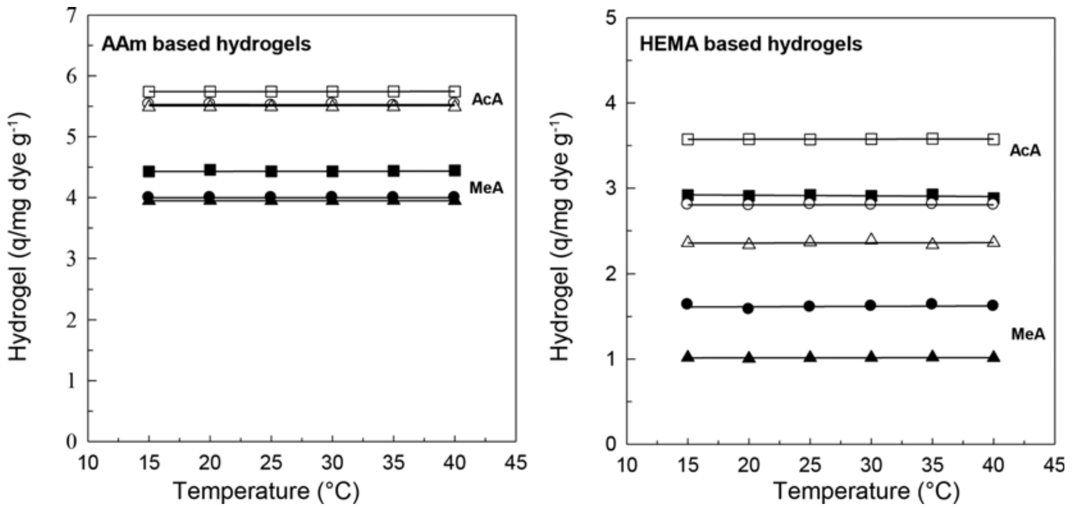

Figure 8. Effect of temperature on dye adsorption onto hydrogels; □; Nile blue, ○; Safranine, △; methylene blue.

the hydrogels at each temperature was calculated. Figure 8 includes the curves that show the variation in the adsorbed amount versus temperature.

The amount of dye adsorbed on the hydrogels did not vary significantly within the temperature range that was examined. Thus, the temperature had no significant effect on the amount of dye adsorbed by the hydrogels within this range.

The study concluded that the relevant AAm- and HEMA-based copolymeric hydrogels can be used to eliminate environmental pollution caused by dyes.

Conclusion

In this work, we investigated the removal of cationic dyes such as safranine, nile blue and methylene blue from aqueous solutions using AAm- or HEMA- based anionic hydrogels.

1. Neutral PAAm or PHEMA hydrogels do not interact with the dye molecules, and adsorption of the dye molecules with the mesaconic and aconitic acid comonomers added to the hydrogels is achieved.
2. AAm- based anionic hydrogels adsorb better the dye molecules than HEMA- based anionic hydrogels.
3. As the number of -COOH groups in the hydrogels increases, the amount of adsorbed material increases.
4. The temperature does not have a significant effect on the amount of dye adsorbed by the hydrogels within this range.
5. Dye adsorption onto the hydrogels was determined to be an *L* type Giles adsorption isotherm.
6. The mass of adsorbents for removal of 50 % of dyes from a hypothetical solution (50 mg l^{-1}) were 0.6-1.6 g l^{-1} for AAm- based hydrogels, and 3.0-9.0 g l^{-1} for HEMA-based hydrogels.
7. It has been determined that the anionic hydrogels will provide dye removal at low cost.

As a result, it can be said that the AAm- or HEMA- based anionic hydrogels can be used effectivelly for the removal of the dyes from aqueous solutions. In particularly, the P(AAm-co-AcA) can be used as cheap and useful adsorbent for dye removal process.

References

1. İ. Karapınar Kabdan and F. Kargı, *Turk. J. Eng. Environ. Sci.*, **24**, 161 (2000).
2. V. V. Panić, S. Šešlija, A. R. Nešić, and S. J. Veličković, *Hem. Ind.,* **6**, 881 (2013).
3. M. Doğan and M. Alkan, *J. Colloid Interface Sci.*, **267**, 32 (2003).
4. T. S. Anirudhan and A. R. Tharun, *Chem. Eng. J.*, **181-**

182, 761 (2012).

5. D. Baybaş and U. Ulusoy, *Turk. J. Chem.*, **40**, 147 (2016).
6. Ö. B. Üzüm and E. Karadağ, *Polym. Plast. Tech. Eng.*, **45**, 1277 (2006a).
7. Ö. B. Üzüm and E. Karadağ, *Adsorpt.*, **12**, 77 (2006b).
8. Ö. B. Üzüm and E. Karadağ, *J. Appl. Polym. Sci.*, **101**, 405 (2006c).
9. T. S. Perova, J. K. Vij, and H. Xu, *Colloid Polym. Sci.*, **275**, 323 (1997).
10. A. Hassani, M. Kiransan, R. Darvishi Cheshmeh Soltani, A. Khataee, and S. Karaca, *Turk. J. Chem.*, **39**, 734 (2015).
11. I. Acar, A. Bal, and G. Güçlü, *Clean-Soil, Air, Water*, **40**, 325 (2012).
12. D. Şolpan, S. Duran, and M. Torun, *Radiat. Phys. and Chem.*, **77**, 447 (2008).
13. S. K. Bajpai, C. Navin, and M. Manika, *Int. J. Environ. Sci.*, **2**, 1609 (2012).
14. M. S. Mohy Eldin, M. H. Gouda, M. E. Youssef, Yehia M. S. El-Shazly, and H. A. Farag, *Fiber. Polym.*, **17**, 1884 (2016).
15. E. Karadağ, D. Saraydın, and Y. Işıkver, *Polym. Plast. Tech. Eng.*, **45**, 729 (2006).
16. E. Karadağ, D. Saraydın, and O. Güven, *Macromol. Mater. Eng.*, **286**, 34 (2001).
17. D. A. Skoog and J. J. Leary, "Principles of Instrumental Analysis", Fort Worth, Tex.: Saunders College Pub., 1992.
18. Y. Işıkver and D. Saraydın, *Polym. Eng. Sci.*, **55**, 843 (2015).
19. D. Baybaş and U. Ulusoy, *J. Hazard. Mater.*, **187**, 241 (2011).
20. T. Çaykara, C. Özyürek, Ö. Kantoğlu, and B. Erdoğan, *Polym. Degrad. Stabil.*, **80**, 339 (2003).
21. W. E. Roorda, J. A. Bouwstra, M. A. de Vries, and H. E. Junjinger, *Pharm. Res.*, **5**, 722 (1988).
22. D. Saraydın, E. Karadağ, Y. Caldiran, and O. Güven, *Radiat. Phys. Chem.*, **60**, 203 (2001).
23. E. Karadağ, D. Saraydin, and O. Güven, *J. Appl. Polym. Sci.*, **66**, 733 (1997).
24. D. Şolpan, S. Duran, D. Saraydin, and O. Güven, *Radiat. Phys. Chem.*, **66**, 117 (2003).
25. H. Guo, T. Jiao, Q. Zhang, W. Guo, Q. Peng, and X. Yan, *Nanoscale Res. Lett.*, **10**, 272 (2015).
26. R. Xing, K. Liu, T. Jiao, N. Zhang, K. Ma, R. Zhang, Q. Zou, G. Ma, and X. Yan, *Adv. Mater.*, **28**, 3669 (2016).
27. R. Xing, T. Jiao, Y. Liu, K. Ma, Q. Zou, G. Ma, and X. Yan, *Polymers*, **8**, 181 (2016).
28. C. H. Giles, T. H. MacEwan, S. N. Nakhwa, and D. Smith, *J. Chem. Soc.*, 3973 (1960).
29. T. B. İyim, I. Acar, and S. Özgümüş, *J. Appl. Polym. Sci.*, **109**, 2774 (2008).
30. G. Güçlü and S. Keleş, *J. Appl. Polym. Sci.*, **106**, 2422 (2007).
31. O. İnel and A. Aşkın Börekçi, *Turk. J. Chem.*, **20**, 276 (1996).
32. M. Doğan, Y. Özdemir, and M. Alkan, *Dyes Pigment.*, **75**, 701 (2007).
33. J. Xiong, J. Tao, K. Guo, C. Jiao, D. Zhang, H. Lin, and Y. Chen, *Fiber. Polym.*, **16**, 1512 (2015).
34. E. Karadağ, D. Saraydın, and O. Güven, *J. Appl. Polym. Sci.*, **61**, 2367 (1996).
35. U. Takahiro, Y. Shuhei, Y. Atsushi, K. Masataka, and I. Takahito, *J. Polym. Sci. Pol. Chem.*, **55**, 1048 (2017).
36. W. Yabo, X. Yi, Z. Yongkui, T. Siyang, G. Chencen, W. Jiansheng, and L. Raymond, *Chem. Eng. Res. Des.*, **114**, 258 (2016).
37. G. Nechifor, D. E. Pascu, M. Pascu, G. A. Traistaru, and P. C. Albu, *U.P.B. Sci. Bull. Series B*, **77**, 63 (2015).